



**Design of Narrow Bandgap Non-Fullerene Acceptors for  
Photovoltaic Applications and Investigation of Non-  
Geminate Recombination Dynamics**

Journal:	<i>Journal of Materials Chemistry C</i>
Manuscript ID	TC-ART-05-2020-002136.R1
Article Type:	Paper
Date Submitted by the Author:	17-Jun-2020
Complete List of Authors:	<p>Vollbrecht, Joachim; Universität Potsdam, Institut für Physik und Astronomie; University of California Santa Barbara, Chemistry and Biochemistry, Center for Polymers and Organic Solids</p> <p>Lee, Jaewon; University of California Santa Barbara, Chemistry and Biochemistry, Center for Polymers and Organic Solids; Pohang University of Science and Technology, Department of Chemical Engineering, Center for Advanced Soft Electronics</p> <p>Ko, Seo-Jin; Korea Research Institute of Chemical Technology</p> <p>Brus, Viktor; UCSB, Center for Polymers and Organic Solids</p> <p>Karki, Akchheta; University of California Santa Barbara, Chemistry and Biochemistry, Center for Polymers and Organic Solids</p> <p>Le, William; University of California Santa Barbara, Chemistry and Biochemistry, Center for Polymers and Organic Solids</p> <p>Seifrid, Martin; University of California Santa Barbara,</p> <p>Ford, Michael; Center for Polymers and Organic Solids, Mitsubishi Chemical - Center for Advanced Materials</p> <p>Cho, Kilwon; Pohang University of Science and Technology, Chemical Engineering</p> <p>Bazan, Guillermo; University of California,</p> <p>Nguyen, Thuc-Quyen; University of California, Santa Barbara, Chemistry and Biochemistry</p>

## **Design of Narrow Bandgap Non-Fullerene Acceptors for Photovoltaic Applications and Investigation of Non-Geminate Recombination Dynamics**

*Joachim Vollbrecht, Jaewon Lee, Seo-Jin Ko, Viktor V. Brus, Akchheta Karki, William Le, Martin Seifrid, Michael J. Ford, Kilwon Cho, Guillermo C. Bazan, Thuc-Quyen Nguyen\**

Dr. J. Vollbrecht, Dr. J. Lee, Dr. V. V. Brus, A. Karki, W. Le, Dr. M. Seifrid, Dr. M. J. Ford,  
Prof. G. C. Bazan, Prof. T.-Q. Nguyen  
Center for Polymers and Organic Solids  
Departments of Chemistry and Biochemistry  
University of California at Santa Barbara  
Santa Barbara, CA 93106, USA  
E-mail: [quyen@chem.ucsb.edu](mailto:quyen@chem.ucsb.edu)

Dr. J. Lee, Prof. K. Cho  
Center for Advanced Soft Electronics  
Department of Chemical Engineering  
Pohang University of Science and Technology  
Pohang, 37673, Republic of Korea

Dr. S.-J. Ko  
Division of Advanced Materials,  
Korea Research Institute of Chemical Technology (KRICT)  
Daejeon 34114, Republic of Korea

*This paper is dedicated to Professor Tobin Marks on the occasion of his 75th birthday.*

Keywords: organic photovoltaics, non-fullerene acceptors, near-infrared optoelectronics, narrow bandgap acceptors, non-geminate recombination

## 1 **Abstract**

2 A new narrow bandgap non-fullerene electron acceptor was designed, synthesized, and  
3 characterized for near-infrared organic photovoltaics. This acceptor was compared to a  
4 structurally similar compound with systematically modified side chains, and a series of solar  
5 cells were fabricated, employing the common donor polymers PTB7-Th and PBDBT. The  
6 devices exhibited charge generation over a wide spectral range and power conversion  
7 efficiencies up to 8.1 %. The non-geminate recombination dynamics were investigated and  
8 quantified *via* a combination of capacitance spectroscopy and transient open-circuit voltage  
9 decay measurements. The reduction of the bandgap results in increased bimolecular  
10 recombination losses, while solar cells composed of PBDBT were afflicted by stronger  
11 monomolecular, i. e. trap-assisted, recombination losses that ultimately caused the lower  
12 power conversion efficiencies of the respective devices. The latter observation could be  
13 correlated to less ordered blend film morphology.

## 14 **1. Introduction**

15 In recent years, organic photovoltaics (OPVs) have received increasing attention  
16 owing to the potential of manufacturing large-area, flexible solar cells *via* mild and  
17 economically favorable solution-based processing techniques.[1, 2] The gains in performance  
18 recently observed for OPVs can mostly be attributed to the use of non-fullerene acceptors  
19 (NFAs) that were developed through continuous efforts to replace the hitherto ubiquitous  
20 fullerene-based acceptors.[3, 4] Organic solar cells (OSCs) based on fullerene acceptors in a  
21 bulk-heterojunction (BHJ) configuration yield power conversion efficiencies (PCEs) of up to  
22 11 % for single-junction devices,[5, 6] while PCEs of over 17 % have been reported for state-  
23 of-the-art, single-junction and tandem NFA-OSCs, placing them within reach of the  
24 performance range of perovskite solar cells.[7-9] In addition to the increased performance,  
25 NFAs can be tuned to yield compounds that absorb at longer wavelengths (e.g., near-

26 infrared).[10, 11] This control over the bandgap opens up the potential to develop semi-  
27 transparent OSCs that could find application in building-integrated photovoltaics and in  
28 agriculture.[12, 13] Even when considering the recent advances in NFAs, it is still necessary  
29 to develop a deeper understanding of loss mechanisms in NFAs such as non-radiative and  
30 non-geminate recombination – the process where free electrons and holes originating from  
31 different excitons recombine – to further improve the performance of OSCs.[14-18] This is  
32 especially required since the interplay between narrow bandgap NFAs ( $E_g \leq 1.3$  eV) and  
33 polymers such as PTB7-Th or PBDBT, originally designed for fullerene acceptors,[19, 20] is  
34 yet not fully understood.[21, 22] Hence, this study focuses on four different narrow bandgap  
35 blend systems in solar cells, the observed photo-physical, morphological, and OPV  
36 performance differences, and how these differences relate to the non-geminate recombination  
37 dynamics.

## 38 2. Results and Discussion

39 We recently reported narrow bandgap electron acceptors, namely CTIC-4F and  
40 COTIC-4F, which are characterized by optical bandgaps ( $E_g^{opt}$ ) of 1.3 and 1.1 eV,  
41 respectively.[11, 23] The molecules are designed based on an A–D'–D–D'–A molecular  
42 configuration, consisting of cyclopentadithiophene (CPDT) as the central donor (D) unit,  
43 thienyl units as the flanked sub-donor (D') fragments, and 2-(5,6-difluoro-3-oxo-2,3-dihydro-  
44 1H-inden-1-ylidene)malononitrile as the terminal acceptor (A) units. The molecular structures  
45 of CTIC-4F and COTIC-4F differ by their side chains on the D' fragments, specifically alkyl  
46 vs. alkoxy groups for CTIC-4F vs. COTIC-4F. Changing the substituent of side chains on the  
47 thienyl fragments is an effective way to modulate the frontier orbital energy levels and  
48 absorption profiles of organic semiconductors.[24, 25] In this work, we designed a new NFA  
49 derivative, namely CETIC-4F (Figure 1), containing a carboxylate substituted group in the 3-  
50 position of the D'-thienyl unit (see Scheme S1, Figures S1-S4). As evidenced by the optical

51 transitions and the cyclic voltammetry, incorporating electron-withdrawing carboxylate  
 52 substituents into alkyl side chains lowers the HOMO level from  $-5.36$  eV for CTIC-4F to  
 53  $-5.47$  eV for CETIC-4F, while resulting in a minor effect on the optical bandgap (Figure 1,  
 54 Figure S5). This underlines the potential of the aforementioned synthetic strategy to finely  
 55 tune the NFAs for energy level matching, while maintaining a similar bandgap.

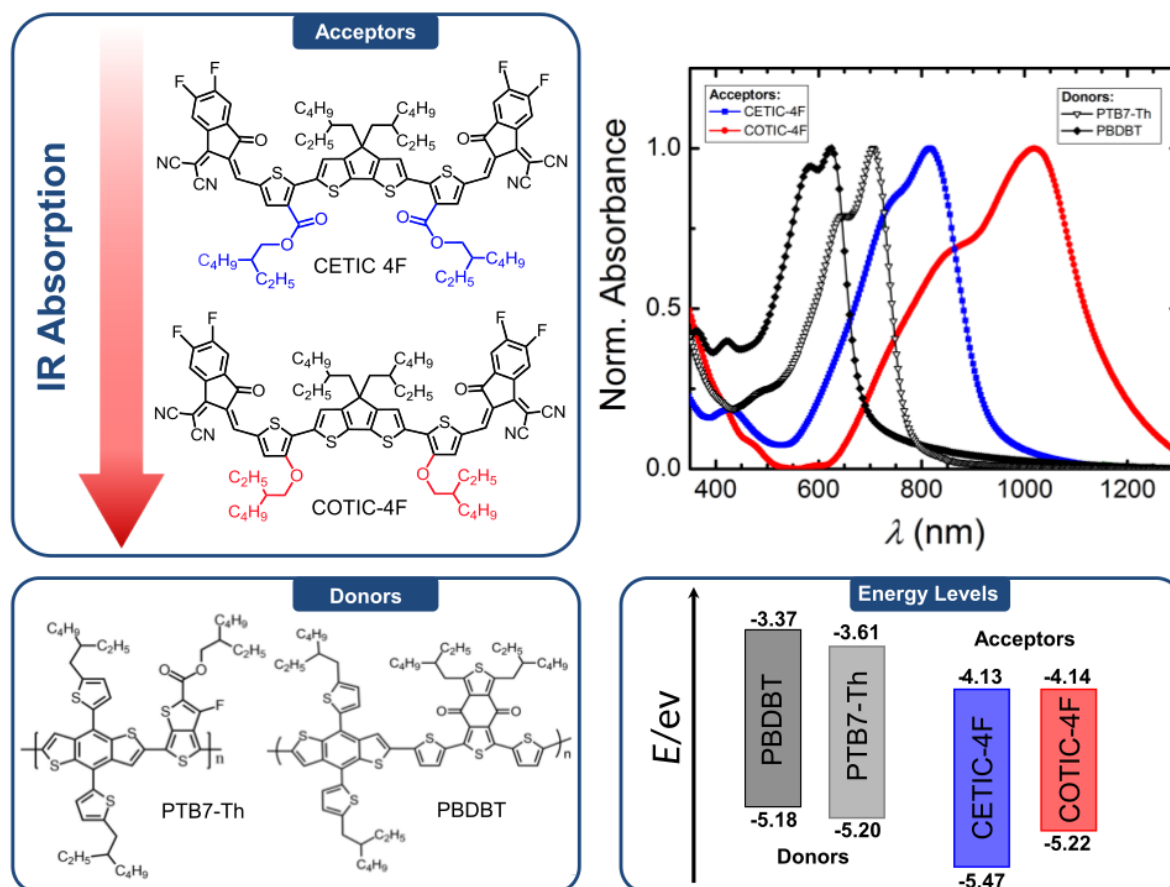


**Figure 1.** Chemical structures of the studied non-fullerene acceptors and donor polymers, absorption spectra of pristine thin films, and relevant energy levels.

56 Organic solar cells were fabricated and optimized to investigate the photovoltaic performance  
 57 of two donors and two NFAs, namely PBDBT and PTB7-Th[19, 20, 26] as well as CETIC-4F  
 58 and COTIC-4F (see ESI).[11, 23] The same trend in performance can be observed for the two  
 59 sets of devices with different donors, where of the investigated NFAs, CETIC-4F shows the  
 60 highest PCE compared to COTIC-4F (see Figure 2, Table 1). Furthermore, the devices with  
 61 PTB7-Th as the donor perform better than their PBDBT counterparts, owing to higher values of

62 the short-circuit current density ( $J_{SC}$ ) and fill factor ( $FF$ ), while in contrast the open-circuit  
 63 voltages ( $V_{OC}$ ) tend to be of a similar value. The COTIC-4F devices showed the biggest drop in  
 64 PCE when changing the donor polymer, namely from up to 7.04 % (PTB7-Th:COTIC-4F) to only  
 65 2.32 % (PBDBT:COTIC-4F). The external quantum efficiency (EQE) measurements reveal that  
 66 PTB7-Th:CETIC-4F and PBDBT:CETIC-4F devices show charge carrier generation in the  
 67 spectral range of 300 – 950 nm, while PTB7-Th:COTIC-4F and PBDBT:COTIC-4F devices  
 68 exhibit charge generation at even longer wavelengths (300 – 1100 nm), which is in good  
 69 agreement with the thin film absorption spectra and earlier reports (Figures 1 and 2).[11]  
 70 Furthermore, the photocurrent density ( $J_{ph}$ ) was calculated, which is defined as follows:

$$71 \quad J_{ph} = J_{light} - J_{dark}, \quad (1)$$

72 where  $J_{light}$  is the current density under illumination and  $J_{dark}$  is the current density in the dark (see  
 73 Figures S6 and S7). The photocurrent density can be compared between the different devices by  
 74 plotting against the effective voltage  $V_{eff} = V_0 - V_{cor}$ , where  $V_0$  is the voltage at which  $J_{ph} = 0$  (Figure  
 75 2) and  $V_{cor}$  is the applied voltage corrected for the losses caused by the series resistance ( $V_{cor} =$   
 76  $V_{app} - J \cdot R_{series}$ ).[27, 28] Similarly, the probability of charge collection  $P_C$  is accessible from the  
 77 ratio between the saturated photocurrent density  $J_{ph,sat}$  with the values for  $J_{ph}$  at different  
 78 biases:[29]

$$79 \quad P_C = \frac{J_{ph}}{J_{ph,sat}}. \quad (2)$$

80 As can be seen in Figure S8, the PTB7-Th:CETIC-4F and PTB7-Th:COTIC-4F devices exhibit  
 81 a better charge collection  $P_C$  than their PBDBT counterparts. When the two NFAs are compared,  
 82 PTB7-Th:CETIC-4F and PBDBT:CETIC-4F devices show a higher  $P_C$  than PTB7-Th:COTIC-4F  
 83 and PBDBT:COTIC-4F devices, respectively; this difference is subtle for the PTB7-Th devices,  
 84 while significant for the PBDBT devices. Ultimately, a reasonable correlation between the  
 85 collection probability  $P_C$  and the device performance can be observed, where higher values for  $P_C$ ,  
 86 specifically at forward bias around maximum-power conditions, go hand in hand with higher

87 values for the solar cell PCEs. Additionally,  $J$ - $V$ -curves at varying light intensities were  
88 measured to qualitatively inspect the non-geminate recombination mechanisms (Figure S9).  
89 The measured  $J_{SC}$  and the light intensity  $I$  follow a power law ( $J_{SC} \propto I^\alpha$ ) and exhibit similar  
90 values for the exponent ( $\alpha \approx 0.9$ ). Bimolecular recombination and space charge effects  
91 resulting from imbalanced hole and electron mobility can both be responsible for such an  
92 observation. Indeed, the hole and electron mobility ( $\mu_{h,e}$ ) obtained *via* single-carrier diodes  
93 analyzed *via* the Mott-Gurney relationship show significant differences in the magnitude of  
94 the two types of mobility for all systems ( $\mu_h/\mu_e = 5 - 138$ , Figure S11 and Table S2). It is  
95 therefore likely that the deviation of the exponent  $\alpha$  from unity is caused by the  
96 aforementioned space charge effect rather than by the influence of bimolecular recombination  
97 alone.[30, 31] The second common approach to investigate the types of non-geminate  
98 recombination mechanisms of solar cells is by determining the relationship between the  $V_{OC}$   
99 and the light intensity  $I$ :[32, 33]

$$100 \quad V_{OC} \propto \frac{kT}{q} \ln(I), \quad (3)$$

101 where  $k$  is the Boltzmann constant,  $T$  is the absolute temperature ( $T = 300$  K), and  $q$  is the  
102 elementary charge.[34] The  $V_{OC}$ - $\ln(I)$ -plots exhibit a slope of  $S = 1 kT/q$  for solar cells in the case  
103 of ideal, pure bimolecular recombination. However, the presence of bulk or surface traps can  
104 cause monomolecular recombination that lead to deviations of the slope (bulk traps:  $S > 1 kT/q$ ;  
105 surface traps:  $S < 1 kT/q$ ).[22, 35, 36] The  $V_{OC}$ - $\ln(I)$ -plots exhibit good linearity over the  
106 investigated light intensities and the slopes determined for the studied devices are in a range of  
107  $S = 0.84 - 1.13 kT/q$ . These results indicate that all types of non-geminate recombination should  
108 be taken into account as loss mechanisms.[36] Hence, the light intensity dependent  $J$ - $V$ -curves are  
109 not sufficient to paint a conclusive picture of the non-geminate recombination dynamics and a  
110 more in-depth analysis is necessary to obtain quantitative results.

**Table 1.** Photovoltaic performance of OSCs with blends consisting of PBDBT or PTB7-Th as donor and CETIC-4F and COTIC-4F as acceptor, measured at simulated 100 mW/cm<sup>2</sup> AM 1.5G illumination.

Donor	NFA	V <sub>oc</sub> [V]	J <sub>sc</sub> [mA/cm <sup>2</sup> ]	FF	PCE <sub>avg (max)</sub> [%] <sup>c)</sup>	J <sub>sc,calc</sub> [mA/cm <sup>2</sup> ] <sup>d)</sup>	EQE <sub>max</sub> [%]
PBDBT <sup>a)</sup>	CETIC-4F	0.71 ± 0.01	15.6 ± 1.1	0.54 ± 0.03	5.96 ± 0.77 (6.59)	15.72	58
	COTIC-4F	0.55 ± 0.03	8.0 ± 0.3	0.49 ± 0.01	2.19 ± 0.12 (2.32)	7.78	26
PTB7-Th <sup>b)</sup>	CETIC-4F	0.65 ± 0.01	19.1 ± 1.0	0.61 ± 0.03	7.61 ± 0.33 (8.08)	18.66	72
	COTIC-4F	0.56 ± 0.01	20.2 ± 0.9	0.59 ± 0.01	6.66 ± 0.17 (7.04)	20.40	57

<sup>a)</sup>PBDBT:NFA blend ratio: 1:1 (w/w); <sup>b)</sup>PTB7-Th:NFA blend ratio: 1:1.5 (w/w); <sup>c)</sup> Average values from 10 devices; <sup>d)</sup>J<sub>sc</sub> calculated from EQE measurements



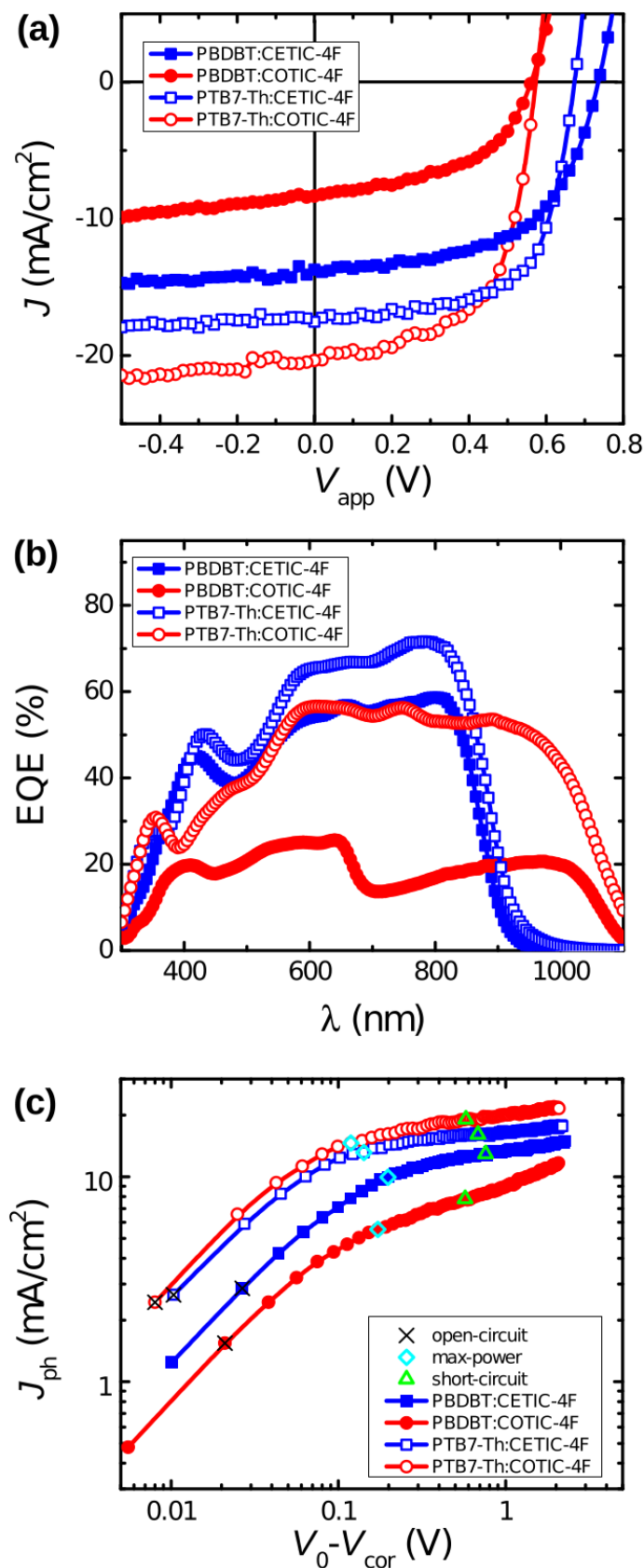


**Figure 2.** (a)  $J$ - $V$ -characteristics, (b) EQE, and (c) photocurrent density  $J_{ph}$  as a function of the effective voltage  $V_0 - V_{cor}$  of the studied solar cells. Operating conditions of interest such as open-circuit, max-power, and short-circuit are highlighted for convenience.

111 The recombination dynamics in the studied solar cells were quantified *via* an analysis based  
 112 on capacitance spectroscopy that allows the determination of the charge carrier density  $n$   
 113 (Equations S3-S5, Figure S12, Figure 3a).[37] The studied solar cells show charge carrier  
 114 densities in a similar range, with the biggest divergence at forward bias approaching open-  
 115 circuit conditions (highest for PTB7-Th:CETIC-4F:  $n = 5.2 \cdot 10^{16} \text{ cm}^{-3}$ ; lowest for  
 116 PBDBT:CETIC-4F:  $n = 2.6 \cdot 10^{16} \text{ cm}^{-3}$ ). To obtain a quantitative understanding of the  
 117 recombination mechanisms, it is assumed that the overall measured recombination current  
 118 density ( $J_{\text{rec}} = J_{\text{ph,sat}} - J_{\text{ph}}$ ) is a superposition of the three aforementioned recombination  
 119 mechanisms that contribute a certain part to the total recombination current density  $J_{\text{rec}}$ :

$$120 \quad J_{\text{rec}} = J_{\text{bm}} + J_{\text{tb}} + J_{\text{ts}} = qL \left( \frac{n}{\tau_{\text{bm}}} + \frac{n}{\tau_{\text{tb}}} + \frac{n}{\tau_{\text{ts}}} \right) = qL(k_{\text{bm}}n^2 + k_{\text{tb}}n + k_{\text{ts}}n), \quad (4)$$

121 where  $q$  is the elementary charge,  $L$  is the active layer thickness,  $\tau$  is the charge carrier  
 122 lifetime,  $n$  is the charge carrier density, and  $k$  is the recombination coefficient of the three  
 123 different recombination mechanisms (bm: bimolecular; tb: bulk trap-assisted; ts: surface trap-  
 124 assisted). By reconstructing the recombination current density  $J_{\text{rec}}$  obtained from the  $J$ - $V$ -  
 125 curves with the charge carrier density ( $n$ ) and the effective mobility ( $\mu_{\text{eff}}$ ), which is explained  
 126 in the ESI, it is possible to quantify the recombination coefficients ( $k$ ) (Figures S13-S15).[22,  
 127 38] In general, the PTB7-Th:COTIC-4F and PBDBT:COTIC-4F devices exhibit higher  
 128 bimolecular recombination coefficients  $k_{\text{bm}}$  than their CETIC-4F-based counterparts.  
 129 Furthermore, the fitting yields higher contributions of bulk trap-assisted recombination in the  
 130 PBDBT:CETIC-4F and PBDBT:COTIC-4F devices compared to the PTB7-Th:CETIC-4F  
 131 and PTB7-Th:COTIC-4F solar cells, which could be the reason for the reduced performance  
 132 of the PBDBT OSCs (Figures S15). In addition, the contributions of surface trap-assisted  
 133 recombination are only relevant under open-circuit conditions for all tested devices and even  
 134 under these conditions they do not dominate the non-geminate recombination dynamics  
 135 (Figure S14).

136 In a subsequent step, it is possible to calculate the charge carrier lifetime  $\tau_{\text{rec}}$  by rearranging  
137 equation (4), since the carrier density  $n$  and the relevant recombination coefficients ( $k_{\text{bm}}$ ,  $k_{\text{tb}}$ ,  
138  $k_{\text{ts}}$ ) are now known (Figure 3b). However, it is necessary to also take the extraction dynamics  
139 of the investigated solar cells into account to obtain a complete picture, since non-geminate  
140 recombination and extraction are in a direct competition to each other (see Equations S6-  
141 S8).[21, 39] To this end, the effective extraction time  $\tau_{\text{ex}}$  can be defined as follows:

$$142 \quad \tau_{\text{ex}} = \frac{qLn}{J}, \quad (5)$$

143 where  $q$  is the elementary charge,  $L$  is the active layer thickness,  $n$  is the charge carrier density,  
144 and  $J$  is the current density (Figure 3b).[38] Once the charge carrier lifetime and the  
145 extraction time are determined, it is possible to calculate the competition factor ( $\theta = \tau_{\text{ex}}/\tau_{\text{rec}}$ ), a  
146 figure of merit introduced by Barthesaghi et al. in 2015.[39] In this study, the bias-dependent  
147 competition factor  $\theta$  is accessible, since the bias-dependent lifetime and extraction time were  
148 determined.[38] In summary, a good reciprocal relationship between the competition factor  $\theta$   
149 and figures of merit for the device performance ( $FF$ ,  $PCE$ ) can be observed (Table 2), where  
150 lower  $\theta$  values go hand in hand with a higher device performance.

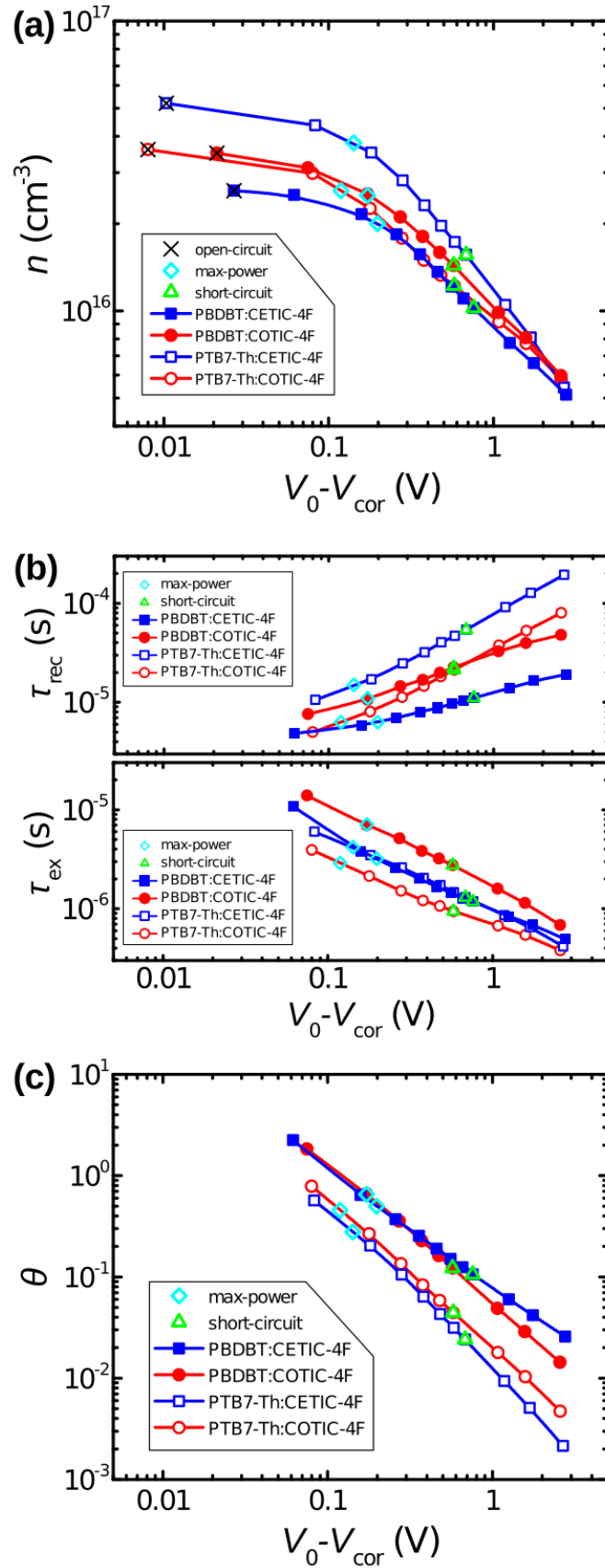


**Figure 3.** (a) Charge carrier density  $n$ , (b) recombination lifetime  $\tau_{rec}$  as well as extraction time  $\tau_{ex}$ , and (c) competition factor  $\theta$  as a function of the effective voltage  $V_0 - V_{cor}$  of the studied solar cell determined *via* capacitance spectroscopy. Operating conditions of interest such as max-power, and short-circuit are highlighted for convenience.

151 In addition to the analysis based on capacitance spectroscopy, we also performed transient  
152 open-circuit voltage decay measurements on the solar cells as a secondary method to  
153 investigate the relevant non-geminate recombination processes (see Equations S9-S14 and  
154 Figure S16). The  $V_{OC}$ -transients depicted convey significant differences between the PTB7-Th  
155 and PBDBT devices (Figure 4a). It takes up to one order of magnitude longer for the  $V_{OC}$  to  
156 drop to half of its initial value for PTB7-Th:CETIC-4F and PTB7-Th:COTIC-4F devices  
157 ( $t_{1/2} = 0.6 - 1.2$  ms), when compared to their PBDBT:CETIC-4F and PBDBT:COTIC-4F  
158 counterparts ( $t_{1/2} = 0.06 - 0.13$  ms; Table 2), which is suggestive of higher recombination rates  
159 in the PBDBT devices. The carrier lifetime  $\tau_{rec}$  and the recombination order  $\beta$  can be determined  
160 from the transients of the  $V_{OC}$  for the relevant timescales not dominated by the shunt resistance  
161 limit (PTB7-Th devices:  $t < 10^{-3}$  s; PBDBT devices:  $t < 10^{-4}$  s, Figure S16). It is revealed that the  
162 highest recombination order  $\beta_{max}$  reached for the PTB7-Th:CETIC-4F and PTB7-Th:COTIC-4F  
163 devices ( $\beta_{max} \approx 1.6$ ) is larger than for the PBDBT:CETIC-4F and PBDBT:COTIC-4F devices  
164 ( $\beta_{max} \approx 1.4$ ) (Equations S11-S14, Figure S16, and Table 2). Another interpretation of the  
165 recombination order  $\beta$  is as an indicator of the relative contribution to the effective recombination  
166 by bimolecular and/or monomolecular recombination.[40] Therefore, higher values of  $\beta_{max}$  result  
167 either from an increased bimolecular contribution, a decreased trap-assisted (e.g. monomolecular)  
168 contribution, or a combination of both cases. To fully quantify the recombination, it is necessary  
169 to transform the measured  $V_{OC}$  values to the transient charge carrier density  $n_{OC}$  and plot the  
170 carrier lifetime  $\tau_{rec}$  against it (Figure 4b,c). Furthermore, it has to be stressed that bulk and surface  
171 trap-assisted recombination cannot be distinguished by this method.[22] The analysis to obtain the  
172 transient carrier density  $n_{OC}$  and the lifetime  $\tau$  is described in detail in the ESI (Equations S11-  
173 S14). In essence the carrier densities under open-circuit conditions determined *via* capacitance  
174 spectroscopy act as a reference point for the transformation of the transient  $V_{OC}$  to the transient  
175  $n_{OC}$  values.[11, 22] Finally, it is possible to obtain values for the different recombination

176 coefficients  $k_{\text{bm}}$  and  $k_{\text{t}}$  (bm: bimolecular; t: trap-assisted) by fitting the relevant parts of the  
 177 measured charge carrier lifetime  $\tau$  (i.e. at high levels of excitation). All studied devices exhibit  
 178 some bimolecular and trap-assisted recombination, which is evidenced by the respective  
 179 recombination coefficients (Table 2).[22] In general, PTB7-Th:COTIC-4F and PBDBT:COTIC-  
 180 4F devices exhibit the highest bimolecular recombination coefficients ( $k_{\text{bm}} \approx 2.0 \cdot 10^{-11} \text{ cm}^3/\text{s}$ ),  
 181 while PTB7-Th:CETIC-4F and PBDBT:CETIC-4F devices show values in a smaller range  
 182 ( $k_{\text{bm}} \approx (0.6 - 1.4) \cdot 10^{-11} \text{ cm}^3/\text{s}$ ). The magnitude of  $k_{\text{bm}}$  is inversely proportional to the bandgap of  
 183 the studied blend system, which correlates with the results obtained *via* capacitance spectroscopy  
 184 and is in agreement with what would be expected from the fundamental relationships governing  
 185 bimolecular recombination.[41] In the case of trap-assisted recombination, PBDBT:CETIC-4F  
 186 and PBDBT:COTIC-4F devices show nearly two orders of magnitude higher values for the  
 187 relevant recombination coefficient ( $k_{\text{t}} \approx 10^5 \text{ s}^{-1}$ ), than the respective PTB7-Th:NFA OSCs  
 188 ( $k_{\text{t}} \approx 10^3 \text{ s}^{-1}$ ).

**Table 2.** Recombination dynamics of OSCs with blends consisting of PBDBT or PTB7-Th as donor and CETIC-4F and COTIC-4F as acceptor.

Donor	NFA	FF	PCE <sub>max</sub> [%]	$\theta_{\text{SC}}$	$\theta_{\text{MP}}$	$t_{1/2}$ [ms]	$\beta_{\text{max}}$	$k_{\text{bm}}$ [cm <sup>3</sup> /s]	$k_{\text{t}}$ [s <sup>-1</sup> ]
PBDBT	CETIC-4F	0.54	6.59	0.1060	0.4997	0.13	1.4	$(0.60 \pm 0.02) \cdot 10^{-11}$	$(9.92 \pm 0.12) \cdot 10^4$
	COTIC-4F	0.49	2.32	0.1226	0.6544	0.06	1.4	$(2.15 \pm 0.05) \cdot 10^{-11}$	$(9.83 \pm 0.19) \cdot 10^4$
PTB7-Th	CETIC-4F	0.61	8.08	0.0241	0.2778	1.20	1.6	$(1.35 \pm 0.02) \cdot 10^{-11}$	$(1.66 \pm 0.07) \cdot 10^3$
	COTIC-4F	0.59	7.04	0.0444	0.4552	0.60	1.7	$(2.06 \pm 0.09) \cdot 10^{-11}$	$(1.54 \pm 0.16) \cdot 10^3$

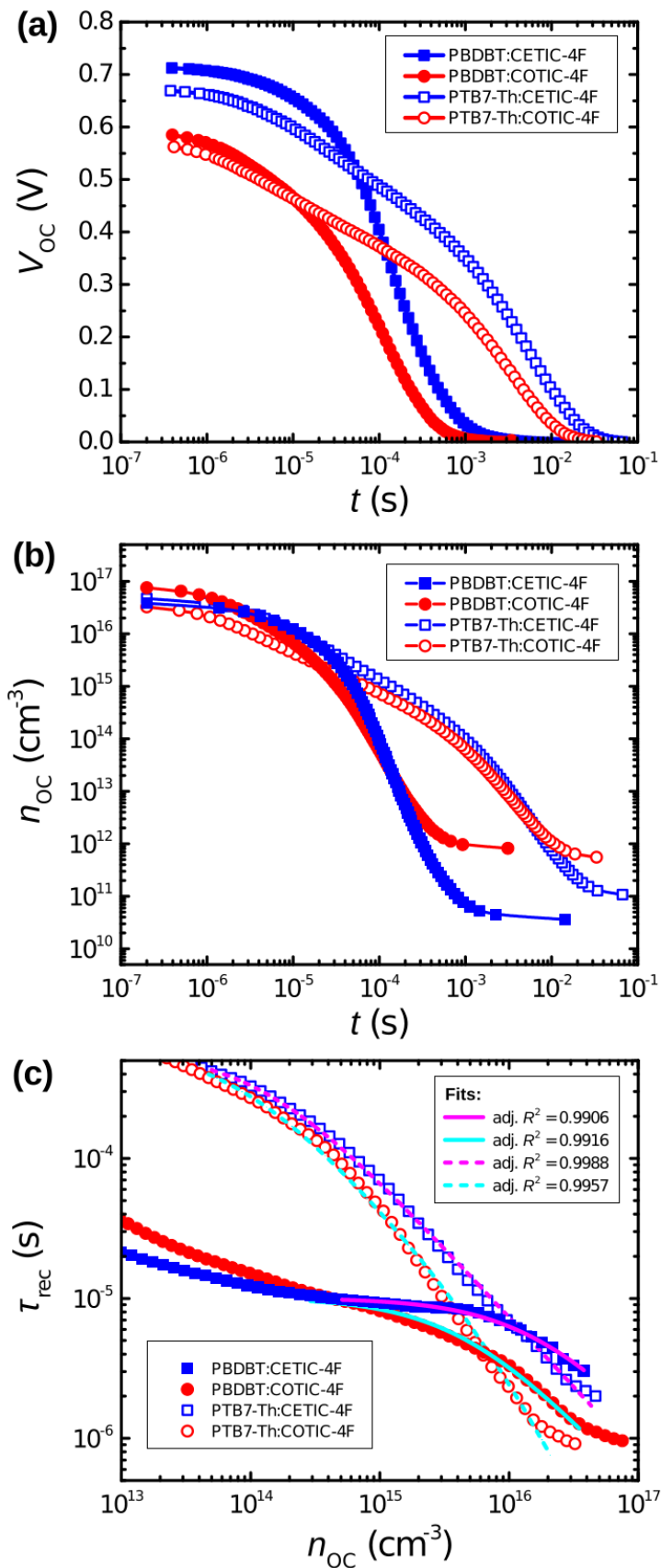


**Figure 4.** (a) Transients of open-circuit voltage  $V_{OC}$  and (b) open-circuit carrier density  $n_{OC}$  of the studied solar cells. (c) Charge carrier lifetime  $\tau_{rec}$  vs. the transient open-circuit carrier density  $n_{OC}$  and their corresponding fits determined *via* open-circuit voltage decay.

189 The investigation of the morphology suggests that the order in the blend films could be  
190 responsible for the differences in trap-assisted recombination and ultimately performance that  
191 were observed for devices with the two studied donor materials. In particular, the  
192 PBDBT:CETIC-4F and PBDBT:COTIC-4F blends show less order in comparison to the PTB7-  
193 Th:CETIC-4F and PTB7-Th:COTIC-4F blends, as evidenced by GIWAXS and AFM  
194 measurements (Figures S17 and S18). The roughness in the AFM measurements is consistently  
195 higher for PBDBT:CETIC-4F and PBDBT:COTIC-4F blends than for the PTB7-Th:CETIC-4F  
196 and PTB7-Th:COTIC-4F blends. GIWAXS measurements show that there are diffraction peaks  
197 from the donor and the acceptor component in the PTB7-Th:CETIC-4F and PTB7-Th:COTIC-4F  
198 blends, while the scattering from PBDBT:CETIC-4F and PBDBT:COTIC-4F blends is  
199 dominated by the polymer. The difference in film composition (60% NFA in PTB7-Th blends and  
200 50% NFA in PBDBT blends) is not likely to account for such a dramatic difference. This suggests  
201 that the NFA domain is significantly less ordered in blends with PBDBT than with PTB7-Th.  
202 Our results show that the difference in trap-assisted recombination is related to whether PTB7-Th  
203 or PBDBT is being used as the donor component of the blend, whereas the difference in  
204 bimolecular recombination is related to the magnitude of the bandgap.

### 205 3. Conclusion

206 In conclusion, the synthesis and characterization of the new NFA CETIC-4F is described and it  
207 was shown that altering the sub-donor (D') fragments is a viable strategy to finely tune the energy  
208 levels. The performance of solar cells based on the common polymer donors PTB7-Th and  
209 PBDBT, as well as the systematically structurally modified NFAs CETIC-4F and COTIC-4F are  
210 investigated. The solar cells exhibited charge generation at wide spectral ranges (300 – 950 nm),  
211 reaching wavelengths as long as 1100 nm in the case of PBDBT:COTIC-4F and PTB7-  
212 Th:COTIC-4F. The PCEs achieved for PTB7-Th:CETIC-4F and PTB7-Th:COTIC-4F devices  
213 (8 %, and 7 %, respectively) were consistently higher than for devices employing



214 PBDBT:CETIC-4F and PBDBT:COTIC-4F (6 %, and 2 %, respectively). This observation could  
215 be linked to considerably higher monomolecular, i.e., bulk trap-assisted recombination losses for  
216 the PBDBT:CETIC-4F and PBDBT:COTIC-4F devices that were determined *via* analyses based  
217 on capacitance spectroscopy and open-circuit voltage decay measurements. AFM and GIWAXS  
218 results indicate that the PBDBT:NFA blend films show higher roughness and less order in  
219 contrast to the PTB7-Th:NFA blends, which likely cause the increased trap-assisted  
220 recombination. Furthermore, PTB7-Th:COTIC-4F and PBDBT:COTIC-4F devices exhibited  
221 higher bimolecular recombination coefficients than their PTB7-Th:CETIC-4F and  
222 PBDBT:CETIC-4F counterparts, which is in agreement with what would be expected from the  
223 fundamental, inverse relationship between the bandgap and bimolecular recombination.

### Acknowledgements

J. V., J. L., and S.-J. K. contributed equally to this work. J.V. acknowledges primary funding by the Alexander-von-Humboldt Stiftung. J.V., V.B., S.-J.K. and T.-Q.N. acknowledge funding by the Office of Naval Research (ONR) grant #N000141410076. J.L. acknowledges funding by the Center for Advanced Soft Electronics under the Global Frontier Research Program (code no. 2011-0031628) of the Ministry of Science and ICT, Korea. X-ray scattering experiments were carried out at the Advanced Light Source, which is a DOE Office of Science user facility under contract no. DE-AC02-05CH11231. We thank Dr. Alexander Mikhailovsky and Ben R. Luginbuhl for assistance with building and testing the measurement setup used for  $V_{OC}$ -decay as well as Jianfei Huang, Sangcheol Yoon, Nora Schopp, Tung Dang Nguyen, Alana Dixon, Álvaro Daniel Romero-Borja, Alexander Lill, Brett Yurash, David Cao and Zhifang Du for fruitful discussions.

**Supporting Information Available:** Additional details about the synthesis, characterization, device fabrication, experimental setups, recombination analysis, and morphological measurements are provided in the Supporting Information.

### References

- [1] Gang Yu, Jun Gao, Jan C Hummelen, Fred Wudl, and Alan J Heeger. Polymer photovoltaic cells: enhanced efficiencies via a network of internal donor-acceptor heterojunctions. *Science*, 270(5243):1789–1791, 1995.
- [2] Luyao Lu, Tianyue Zheng, Qinghe Wu, Alexander M Schneider, Donglin Zhao, and Luping Yu. Recent advances in bulk heterojunction polymer solar cells. *Chemical reviews*, 115(23):12666–12731, 2015.
- [3] Chen Li and Henrike Wonneberger. Perylene imides for organic photovoltaics: yesterday, today, and tomorrow. *Advanced Materials*, 24(5):613–636, 2012.

- [4] Guangye Zhang, Jingbo Zhao, Philip CY Chow, Kui Jiang, Jianquan Zhang, Zonglong Zhu, Jie Zhang, Fei Huang, and He Yan. Nonfullerene acceptor molecules for bulk heterojunction organic solar cells. *Chemical reviews*, 118(7):3447–3507, 2018.
- [5] Jingbo Zhao, Yunke Li, Guofang Yang, Kui Jiang, Haoran Lin, Harald Ade, Wei Ma, and He Yan. Efficient organic solar cells processed from hydrocarbon solvents. *Nature Energy*, 1(2):15027, 2016.
- [6] Yaocheng Jin, Zhiming Chen, Manjun Xiao, Jiajun Peng, Baobing Fan, Lei Ying, Guichuan Zhang, Xiao-Fang Jiang, Qingwu Yin, Ziqi Liang, Fei Huang, and Yong Cao. Thick film polymer solar cells based on naphtho [1, 2-c: 5, 6-c] bis [1, 2, 5] thiadiazole conjugated polymers with efficiency over 11%. *Advanced Energy Materials*, 7(22):1700944, 2017.
- [7] Lingxian Meng, Yamin Zhang, Xiangjian Wan, Chenxi Li, Xin Zhang, Yanbo Wang, Xin Ke, Zuo Xiao, Liming Ding, Ruoxi Xia, Hin-Lap Yip, Yong Cao, and Yongsheng Chen. Organic and solution-processed tandem solar cells with 17.3% efficiency. *Science*, 361(6407):1094–1098, 2018.
- [8] Nicola Gasparini, Alberto Salleo, Iain McCulloch, and Derya Baran. The role of the third component in ternary organic solar cells. *Nature Reviews Materials*, 4:229–242, 2019.
- [9] Yong Cui, Huifeng Yao, Jianqi Zhang, Kaihu Xian, Tao Zhang, Ling Hong, Yuming Wang, Ye Xu, Kangqiao Ma, Cunbin An, Chang He, Zhixiang Wei, Feng Gao, and Jianhui Hou. Single-junction organic photovoltaic cells with approaching 18% efficiency. *Advanced Materials*, page 1908205, 2020.
- [10] Jianfei Huang, Jaewon Lee, Joachim Vollbrecht, Viktor V Brus, Alana L Dixon, David Xi Cao, Ziyue Zhu, Zhifang Du, Hengbin Wang, Kilwon Cho, et al. A high-performance solution-processed organic photodetector for near-infrared sensing. *Advanced Materials*, 32(1):1906027, 2019.
- [11] Jaewon Lee, Seo-Jin Ko, Hansol Lee, Jianfei Huang, Ziyue Zhu, Martin Seifrid, Joachim Vollbrecht, Viktor V Brus, Akchheta Karki, Hengbin Wang, et al. Side chain engineering of non-fullerene acceptors for near-infrared organic photodetectors and photovoltaics. *ACS Energy Letters*, 4(6):1401–1409, 2019.
- [12] Richard R Lunt and Vladimir Bulovic. Transparent, near-infrared organic photovoltaic solar cells for window and energy-scavenging applications. *Applied Physics Letters*, 98(11):61, 2011.
- [13] Viktor V Brus, Jaewon Lee, Ben Luginbuhl, Seo-Jin Ko, Guillermo C Bazan, and Thuc-Quyen Nguyen. Solution-processed semitransparent organic photovoltaics: From molecular design to device performance. *Advanced Materials*, 31(30):1900904, 2019.
- [14] Mohammed Azzouzi, Jun Yan, Thomas Kirchartz, Kaikai Liu, Jinliang Wang, Hongbin Wu, and Jenny Nelson. Nonradiative energy losses in bulk-heterojunction organic photovoltaics. *Physical Review X*, 8(3):031055, 2018.
- [15] Michelle S Vezie, Mohammed Azzouzi, Andrew M Telford, Thomas R Hopper, Alexander B Sieval, Jan C Hummelen, Kealan Fallon, Hugo Bronstein, Thomas Kirchartz, Artem A Bakulin, et al. Impact of marginal exciton–charge-transfer state offset on charge generation and recombination in polymer: Fullerene solar cells. *ACS Energy Letters*, 4(9):2096–2103, 2019.
- [16] Hyojung Cha, Scot Wheeler, Sarah Holliday, Stoichko D Dimitrov, Andrew Wadsworth, Hyun Hwi Lee, Derya Baran, Iain McCulloch, and James R Durrant. Influence of blend morphology and energetics on charge separation and recombination dynamics in organic solar cells incorporating a nonfullerene acceptor. *Advanced Functional Materials*, 28(3):1704389, 2018.
- [17] Ching-Hong Tan, Jeffrey Gorman, Andrew Wadsworth, Sarah Holliday, Selvam Subramaniyan, Samson A Jenekhe, Derya Baran, Iain McCulloch, and James R Durrant. Barbiturate end-capped non-fullerene acceptors for organic solar cells: tuning acceptor

energetics to suppress geminate recombination losses. *Chemical communications*, 54(24):2966–2969, 2018.

[18] Derya Baran, Nicola Gasparini, Andrew Wadsworth, Ching Hong Tan, Nimer Wehbe, Xin Song, Zeinab Hamid, Weimin Zhang, Marios Neophytou, Thomas Kirchartz, Christoph J Brabec, James R Durrant, and Iain McCulloch. Robust nonfullerene solar cells approaching unity external quantum efficiency enabled by suppression of geminate recombination. *Nature communications*, 9(1):1–9, 2018.

[19] Zhicai He, Biao Xiao, Feng Liu, Hongbin Wu, Yali Yang, Steven Xiao, Cheng Wang, Thomas P Russell, and Yong Cao. Single-junction polymer solar cells with high efficiency and photovoltage. *Nature Photonics*, 9(3):174, 2015.

[20] Deping Qian, Long Ye, Maojie Zhang, Yongri Liang, Liangjie Li, Ye Huang, Xia Guo, Shaoqing Zhang, Zhan<sup>TM</sup> Mao Tan, and Jianhui Hou. Design, application, and morphology study of a new photovoltaic polymer with strong aggregation in solution state. *Macromolecules*, 45(24):9611–9617, 2012.

[21] Michael C Heiber, Takashi Okubo, Seo-Jin Ko, Benjamin R Luginbuhl, Niva Ran, Ming Wang, Hengbin Wang, Mohammad Afsar Uddin, Han Young Woo, Guillermo C Bazan, et al. Measuring the competition between bimolecular charge recombination and charge transport in organic solar cells under operating conditions. *Energy & Environmental Science*, 11:3019–3032, 2018.

[22] Joachim Vollbrecht, Viktor V Brus, Seo-Jin Ko, Jaewon Lee, Akchheta Karki, David Xi Cao, Kilwon Cho, Guillermo C Bazan, and Thuc-Quyen Nguyen. Quantifying the nongeminate recombination dynamics in nonfullerene bulk heterojunction organic solar cells. *Advanced Energy Materials*, 9(32):1901438, 2019.

[23] Jaewon Lee, Seo-Jin Ko, Martin Seifrid, Hansol Lee, Benjamin R Luginbuhl, Akchheta Karki, Michael Ford, Katie Rosenthal, Kilwon Cho, Thuc-Quyen Nguyen, et al. Bandgap narrowing in non-fullerene acceptors: Single atom substitution leads to high optoelectronic response beyond 1000 nm. *Advanced Energy Materials*, 8(24):1801212, 2018.

[24] Maojie Zhang, Xia Guo, Wei Ma, Harald Ade, and Jianhui Hou. A polythiophene derivative with superior properties for practical application in polymer solar cells. *Advanced Materials*, 26(33):5880–5885, 2014.

[25] Lijun Huo, Yi Zhou, and Yongfang Li. Alkylthio-substituted polythiophene: absorption and photovoltaic properties. *Macromolecular rapid communications*, 30(11):925–931, 2009.

[26] Akchheta Karki, Gert-Jan AH Wetzelaer, Gollapalli Narayana Manjunatha Reddy, Vojtech Nádaždy, Martin Seifrid, Franz Schauer, Guillermo C Bazan, Bradley F Chmelka, Paul WM Blom, and Thuc-Quyen Nguyen. Unifying energetic disorder from charge transport and band bending in organic semiconductors. *Advanced Functional Materials*, 29(20):1901109, 2019.

[27] Viktor V Brus, Christopher M Proctor, Niva A Ran, and Thuc-Quyen Nguyen. Capacitance spectroscopy for quantifying recombination losses in nonfullerene small-molecule bulk heterojunction solar cells. *Advanced Energy Materials*, 6(11):1502250, 2016.

[28] Joachim Vollbrecht, Christian Wiebeler, Harald Bock, Stefan Schumacher, and Heinz-Siegfried Kitzerow. Curved polar dibenzocoronene esters and imides versus their planar centrosymmetric homologs: Photophysical and optoelectronic analysis. *The Journal of Physical Chemistry C*, 123:4483–4492, 2019.

[29] Aung Ko Ko Kyaw, Dong Hwan Wang, David Wynands, Jie Zhang, Thuc-Quyen Nguyen, Guillermo C Bazan, and Alan J Heeger. Improved light harvesting and improved efficiency by insertion of an optical spacer (zno) in solution-processed small-molecule solar cells. *Nano letters*, 13(8):3796–3801, 2013.

- [30] Sarah R Cowan, Natalie Banerji, Wei Lin Leong, and Alan J Heeger. Charge formation, recombination, and sweep-out dynamics in organic solar cells. *Advanced Functional Materials*, 22(6):1116–1128, 2012.
- [31] LJA Koster, VD Mihailetschi, H Xie, and PWM Blom. Origin of the light intensity dependence of the short-circuit current of polymer/fullerene solar cells. *Applied Physics Letters*, 87(20):203502, 2005.
- [32] Christopher M Proctor, Martijn Kuik, and Thuc-Quyen Nguyen. Charge carrier recombination in organic solar cells. *Progress in Polymer Science*, 38(12):1941–1960, 2013.
- [33] Mohammed Azzouzi, Thomas Kirchartz, and Jenny Nelson. Factors controlling open-circuit voltage losses in organic solar cells. *Trends in Chemistry*, 1(1):49–62, 2019.
- [34] L Jan A Koster, Valentin D Mihailetschi, R Ramaker, and Paul WM Blom. Light intensity dependence of open-circuit voltage of polymer: fullerene solar cells. *Applied physics letters*, 86(12):123509, 2005.
- [35] MM Mandoc, FB Kooistra, JC Hummelen, B De Boer, and PWM Blom. Effect of traps on the performance of bulk heterojunction organic solar cells. *Applied Physics Letters*, 91(26):263505, 2007.
- [36] VV Brus. Light dependent open-circuit voltage of organic bulk heterojunction solar cells in the presence of surface recombination. *Organic Electronics*, 29:1–6, 2016.
- [37] Christopher M Proctor, Chunki Kim, Dieter Neher, and Thuc-Quyen Nguyen. Nongeminate recombination and charge transport limitations in diketopyrrolopyrrole-based solution-processed small molecule solar cells. *Advanced Functional Materials*, 23(28):3584–3594, 2013.
- [38] Akchheta Karki, Joachim Vollbrecht, Alana L Dixon, Nora Schopp, Max Schrock, GN Manjunatha Reddy, and Thuc-Quyen Nguyen. Understanding the high performance of over 15% efficiency in single-junction bulk heterojunction organic solar cells. *Advanced Materials*, 31(48):1903868, 2019.
- [39] Davide Bartesaghi, Irene del Carmen Pérez, Juliane Kniepert, Steffen Roland, Mathieu Turbiez, Dieter Neher, and L Jan Anton Koster. Competition between recombination and extraction of free charges determines the fill factor of organic solar cells. *Nature communications*, 6:7083, 2015.
- [40] Viktor V Brus, Felix Lang, Jürgen Bundesmann, Sophie Seidel, Andrea Denker, Bernd Rech, Giovanni Landi, Heinz C Neitzert, Jörg Rappich, and Norbert H Nickel. Defect dynamics in proton irradiated ch<sub>3</sub>nh<sub>3</sub>pb<sub>3</sub> perovskite solar cells. *Advanced Electronic Materials*, 3(2):1600438, 2017.
- [41] W Van Roosbroeck and W Shockley. Photon-radiative recombination of electrons and holes in germanium. *Physical Review*, 94(6):1558, 1954.

ToC figure

